

“Di-Neutron” Configuration of ${}^6\text{He}$

Yu. Ts. Oganessian and V. I. Zagrebaev

Flerov Laboratory of Nuclear Reaction, JINR, Dubna, Moscow Region, Russia

J. S. Vaagen

SENTEF, Institute of Physics, University of Bergen, N-5007 Bergen, Norway

(Received 18 December 1998)

Two-neutron transfer reactions induced by the Borromean nucleus ${}^6\text{He}$ on ${}^4\text{He}$ and ${}^1\text{H}$ targets are analyzed within a realistic four-body model. Available experimental data are well described, and it is the “di-neutron” configuration of the ${}^6\text{He}$ nucleus that is found to make the dominant contribution to the cross sections of the two-neutron transfer reactions. [S0031-9007(99)09437-5]

PACS numbers: 25.60.Je, 24.10.Eq, 25.10.+s, 27.20.+n

Among the neutron drip-line nuclei there are the very interesting cases of the Borromean nuclei consisting of an inert core and two valence neutrons which cannot bind to the core separately but only as a pair. The n - n correlations lead to the formation of a two-neutron halo structure observed in ${}^6\text{He}$, ${}^{11}\text{Li}$, and ${}^{14}\text{Be}$. Although experiments with secondary radioactive beams have focused much on the properties of ${}^{11}\text{Li}$, the case of ${}^6\text{He}$ can be even more interesting both from the experimental and theoretical points of view. In particular, the “di-neutron” and “cigarlike” configurations, predicted for ${}^6\text{He}$ ground state (g.s.) structure [1] await further experimental exploration. Good understanding of the two-neutron correlations in ${}^6\text{He}$ will allow us to study more confidently the multineutron correlations in heavier helium isotopes and in other light neutron-rich nuclei.

Transfer reactions provide a good tool for studying the structural parameters and spectroscopic factors of nuclear configurations such as contained in the ${}^6\text{He}$ g.s. wave function. The energy region of 10–30 MeV/nucleon seems to be favorable for few-nucleon transfer reactions induced by light exotic nuclei. In slow collisions (≤ 5 MeV/nucleon) a strong channel coupling can significantly complicate the reaction mechanism and prevent simple theoretical models and unambiguous conclusions. For higher collision energies the probability of transfer processes becomes less and less. Furthermore, simple reaction mechanisms should play a dominant role in transfer processes if light targets of simple structure are used. Experimental results have recently been obtained at FLNR (Dubna) on the reaction of $2n$ transfer in collisions of ${}^6\text{He}$ with ${}^4\text{He}$ and ${}^1\text{H}$ targets at beam energy of 151 MeV [2,3]. In this Letter we present the main results of our analysis of these experimental data with the focus on new direct information on the structure of the halo nucleus ${}^6\text{He}$, in particular, on the role of its di-neutron configuration.

In describing reactions with Borromean nuclei (such as ${}^6\text{He}$) we take advantage of their predominant few-body structure, but still we have to consider the combined motion of no less than four particles: target nucleus + projectile consisting of a core and two halo nucleons. We

cannot yet solve the Schrödinger equation exactly with realistic two-body interaction potentials. At sufficiently high energies (above 20 MeV/nucleon) the direct reaction mechanisms should dominate and the distorted-wave Born approximation (DWBA) (with well-determined initial and final asymptotic states and a realistic transfer interaction) is known to be applicable for a description of $1n$ - and $2n$ -transfer reactions [4]. So, we restrict the degrees of freedom by considering a four-body system and restrict the reaction dynamics to the contribution of only a one-step direct reaction mechanism.

The two nucleon transfer reaction can be written as $1 + [2(34)] \rightarrow [1(34)] + 2$. The motion of two valence nucleons (3 and 4) is of special interest in Borromean nuclei. In the entrance channel the coordinate set $(\mathbf{x}, \mathbf{y}_i, \mathbf{R}_i)$ is most convenient for calculation of the incoming distorted wave $\chi_i^{(+)}(\mathbf{R}_i)$ and the three-body bound state wave function of the projectile $\Psi_i^{(234)}(\mathbf{x}, \mathbf{y}_i)$; here \mathbf{x} is the vector between the two valence nucleons and \mathbf{y}_i describes the relative position of the nucleon pair and the core. A thorough understanding of the exotic genuine few-body structure of halo nuclei is of prime interest. For that purpose we use accurately calculated three-body bound state wave functions $\Psi_i^{(234)}(\mathbf{x}, \mathbf{y})$ (core + N + N) making an expansion over hyperspherical harmonics and solving numerically the coupled Schrödinger equations [1,5].

We write the transition amplitude in standard DWBA form

$$T_{fi}^{\text{DWBA}} = \sqrt{S_i S_f} \langle \chi_{\mathbf{k}_f}^{(-)} \Psi_f^{(134)} | \Delta V | \Psi_i^{(234)} \chi_{\mathbf{k}_i}^{(+)} \rangle, \quad (1)$$

where ΔV is the transfer interaction taken in the post ($V_{23} + V_{24} + V_{12} - U_f^{\text{OM}}$) or prior ($V_{13} + V_{14} + V_{12} - U_i^{\text{OM}}$) form which are identical in the case of ${}^6\text{He} + {}^4\text{He}$ collision. This DWBA transition amplitude is a nine-dimensional integral which takes into account the intrinsic three-body motion in the projectile and ejectile and should be evaluated accurately to understand the influence of the internal structure of the loosely bound projectile on the reaction dynamics. Thus, we may be

able to obtain information concerning the internal structure of Borromean nuclei directly from the analysis of experimental $2n$ transfer cross sections. We calculate the nine-dimensional integral (1) explicitly (without serious simplifications) by integrating directly over \mathbf{x} , \mathbf{y}_i , and \mathbf{R}_i , i.e., without partial wave decomposition of the distorted waves. The halo neutrons may also be transferred sequentially—one by one, but the nature of the Borromean nucleus itself (absence of two-body bound state in ${}^5\text{He}$ and strong neutron-neutron correlations) makes us believe that the simultaneous transfer of the neutrons is a major part of the two-neutron transfer reactions induced by ${}^6\text{He}$. In (1) S_i and S_f are the spectroscopic factors giving the weights of the three-body configuration (i.e., inert core plus two nucleons) in the ground state of the projectile nucleus [2(3,4)] and in the residual nucleus [1(3,4)], correspondingly. For a real halo nucleus this spectroscopic factor should be close to unity (a necessary but not sufficient condition for the formation of a nuclear halo). Thus, comparison of the absolute values of experimental and calculated two-neutron transfer cross sections already allows us to probe if the nucleus under study has a three-cluster form—an inert core plus two nucleons. For the ${}^6\text{He}$ nucleus this seems natural due to the compact α -particle core, but for heavier exotic nuclei (even the Borromean ones) it should be tested separately.

Figure 1 shows the spatial correlation density plot for the ground state of ${}^6\text{He}$,

$$P(x, y) = x^2 y^2 \int |\Psi_i^{(234)}(\mathbf{x}, \mathbf{y})|^2 d\Omega_x d\Omega_y. \quad (2)$$

The plot exhibits two prominent peaks: a “di-neutronlike” peak with the two valence neutrons located together well outside the α particle and a cigarlike peak with the valence neutrons positioned on opposite sides of the α particle. These configurations are shown schematically in the inset of Fig. 1. A “direct” experimental observation of this two-component structure of ${}^6\text{He}$, a “filter” which could determine their relative weights, would be of great interest. Their origin is connected with dominance of $L = S = 0$ motion in the 0^+ g.s. of ${}^6\text{He}$ and the Pauli principle blocking the s motion and making the valence nucleons fill the $1p$ state in a shell model picture. This is especially clear

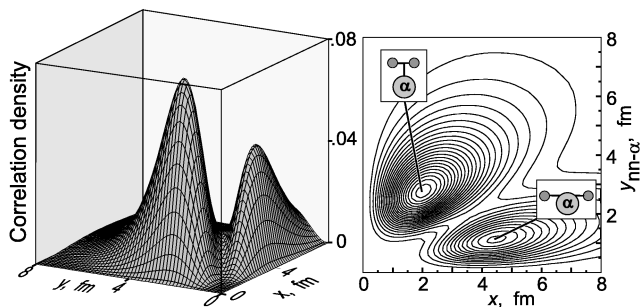


FIG. 1. Spatial correlation density plot for the 0^+ ground state of ${}^6\text{He}$. Two components—di-neutron and cigarlike—are shown schematically.

within the cluster-orbital shell model approximation [1]. Switching off the neutron-neutron interaction and introducing one-particle oscillator functions for the neutron-core relative motion $f_{1p}(r_k) \sim r_k \exp(-\beta r_k^2)$ ($k = 1, 2$) we easily find for $L = S = 0$,

$$\Psi^{00} \sim (\mathbf{r}_1 \cdot \mathbf{r}_2) e^{-\beta(r_1^2 + r_2^2)} = \left[y^2 - \left(\frac{x}{2} \right)^2 \right] e^{-2\beta[y^2 + (\frac{x}{2})^2]}. \quad (3)$$

So, in the absence of V_{nn} there are two distinguishable maxima of equal heights in the ${}^6\text{He}$ bound state wave function and only the neutron-neutron interaction makes the di-neutron component more pronounced.

To find the contributions of these two components in the $2n$ transfer cross section we have to somehow project the total wave function $\Psi_{{}^6\text{He}}(\mathbf{x}, \mathbf{y})$ onto the di-neutron and cigarlike configurations. As can be seen from Fig. 1 and Eq. (3) the two configurations are located on different sides of the line $y = x/2$. Entering the coordinate $\xi = (x/2 - y)/\sqrt{1 + 1/4}$ which changes along the path orthogonal to the separating line $y = x/2$, we may define the operators $\hat{P}_{\text{di-n}} = [1 + \exp(\xi/\xi_0)]^{-1}$ and $\hat{P}_{\text{cig}} = 1 - \hat{P}_{\text{di-n}}$, which approximately divide the total tree-body wave function into the di-neutron and cigarlike parts

$$\Psi_{{}^6\text{He}}(\mathbf{x}, \mathbf{y}) = \Psi_{{}^6\text{He}}^{\text{di-n}} + \Psi_{{}^6\text{He}}^{\text{cig}} \equiv \hat{P}_{\text{di-n}} \Psi_{{}^6\text{He}} + \hat{P}_{\text{cig}} \Psi_{{}^6\text{He}}. \quad (4)$$

To avoid the artificial oscillations that a sharp cutoff would introduce, we use the Fermi-type projection given above. The overlap of the two components is found to be less than 12% if we choose $\xi_0 = 0.65$ fm or less; see Fig. 2.

Experimental data on the elastic scattering of ${}^6\text{He} + {}^4\text{He}$ at the beam energy of 151 MeV are shown in Fig. 3. To analyze these results, we first described the forward angle data within the standard optical model (OM). Unfortunately, forward angle elastic scattering cross sections are available only in the rather narrow center-of-mass angular region $17^\circ - 59^\circ$. A fitting of these data does not give reliable OM potential parameters. Instead, we took as our starting point the OM potential previously found for the case of ${}^6\text{Li} + {}^4\text{He}$ elastic scattering at $E_{\text{c.m.}} = 99.6$ MeV

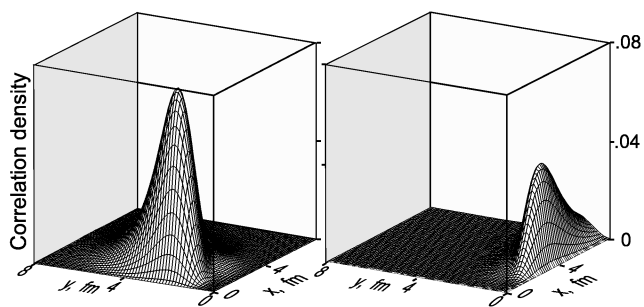


FIG. 2. Correlation density plots for the ground state of ${}^6\text{He}$ projected onto the di-neutron (left) and cigarlike (right) configurations—Eq. (4).

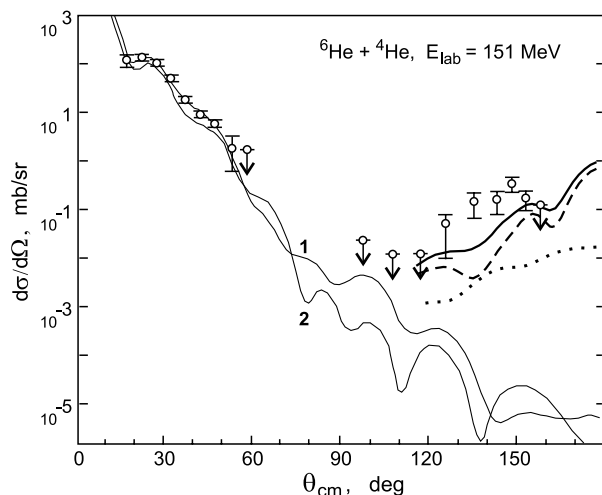


FIG. 3. The ${}^6\text{He} + {}^4\text{He}$ elastic scattering at $E_{\text{lab}} = 151$ MeV. The thin curves 1 and 2 show the potential scattering (see text). The thick solid line corresponds to the $2n$ exchange process, whereas the dashed and dotted lines show the contributions of the di-neutron and cigarlike configurations of ${}^6\text{He}$ to the $2n$ -transfer process.

[6]. With a small variation of these OM potential parameters we were able to obtain a rather good fit of the forward angle data; see curve 1 in Fig. 3 and set 1 of Table I. Experimental data for elastic scattering in a wider forward angle region are desirable for final conclusions regarding the OM potential parameters of the ${}^6\text{He} + {}^4\text{He}$ interaction. The elastic scattering cross section with the real double-folding potential proposed by Baye *et al.* [7] for the ${}^6\text{He} + {}^4\text{He}$ interaction and an imaginary OMP part, that of set 1 (Table I) is shown by curve 2 in Fig. 3.

At the backward angular range of 130° – 160° the experimental elastic scattering cross section is about 3 orders of magnitude larger than that calculated with standard OM code. As was expected, no reasonable set of OM parameters could reproduce the yield of the ${}^6\text{He}$ nuclei observed in the backward direction at such a high incident energy. This definitely means that the ${}^6\text{He}$ elastic scattering events observed in this backward angular region are in fact the result of two-neutron exchange with the ${}^4\text{He}$ target-nucleus.

Using the OM parameters of Table I (set 1) and a spin-independent interaction $V_{23} = V_{24} = V_{an}$ of Gaussian shape with depth of -47 MeV and width $b = 2.4$ fm (the spin-orbital part of this interaction is much less and gives

a much smaller contribution to the transfer cross section), we have calculated the cross section of the $2n$ transfer process in the reaction ${}^4\text{He}({}^6\text{He}, {}^4\text{He}){}^6\text{He}(\text{g.s.})$ within our four-body three-dimensional approach. The resulting $2n$ exchange cross section is shown in Fig. 3 by the thick solid curve. By slightly varying the OM parameters and (or) the parameters of the transfer interaction ΔV we may obtain a somewhat better fit to the backward-angle experimental data. We did not pursue this because of rather large experimental errors and experimental reaction cross sections which for the time being are limited to the angular interval of 125° – 158° . Instead of aiming at a precise fitting of the available experimental data, we have tried to elucidate the dynamics of the reaction and the sensitivity of the $2n$ transfer cross section to the double-component structure of ${}^6\text{He}$.

Inserting the wave functions $\Psi_{6\text{He}}^{\text{di-}n} = \hat{P}_{\text{di-}n}\Psi_{6\text{He}}$ and $\Psi_{6\text{He}}^{\text{cig}} = \hat{P}_{\text{cig}}\Psi_{6\text{He}}$ separately into the transition amplitude (1) instead of $\Psi_f^{(134)}(\mathbf{x}, \mathbf{y}_f)$ and retaining the total wave function $\Psi_i^{(234)}(\mathbf{x}, \mathbf{y}_i)$ (to keep the normalization), we found the contributions of the di-neutron and cigarlike configurations to the $2n$ transfer cross section of the ${}^4\text{He}({}^6\text{He}, {}^4\text{He}){}^6\text{He}$ reaction shown in Fig. 3. The contributions of the two components are quite different. At backward angles the di-neutron configuration of ${}^6\text{He}$ determines the two-neutron transfer reaction. This fact reflects a larger weight of this configuration in the ground state of ${}^6\text{He}$ and a predominant surface localization of the $2n$ transfer process leading to forward emission of the ejectiles. With increasing transferred momentum the contribution of smaller impact parameters to the transfer cross section becomes larger and the role of the cigarlike configuration located near to the core increases—Fig. 3.

A hydrogen target may be the most preferable for studying the structure and spatial configurations of exotic nuclei at medium energies. The short range of proton-neutron interaction and sufficiently small radius of ${}^3\text{H}$ should lead to a much higher selectivity of transfer reactions to the two spatial configurations in ${}^6\text{He}$. We may expect, for example, that in peripheral collisions only closely located neutrons in ${}^6\text{He}$ could be captured by the proton (with formation of ${}^3\text{H}$) with a large probability. The measured [3] $2n$ transfer cross section in the ${}^1\text{H}({}^6\text{He}, {}^4\text{He}){}^3\text{H}$ reaction at beam energy of 151 MeV is compared in Fig. 4 with the deuteron transfer in the ${}^6\text{Li}(p, {}^3\text{He}){}^4\text{He}$ reaction obtained previously in [8] at just the same energy.

TABLE I. Optical model parameters.

Set	$E_{\text{c.m.}}$ (MeV)	V_0^{vol} (MeV)	R_V (fm)	a_V (fm)	W_0^{vol} (MeV)	R_W (fm)	a_W (fm)
1, ${}^6\text{He} + {}^4\text{He}$	60.4	-102.5	1.78	0.920	-13.0	3.85	0.500
2, ${}^6\text{He} + {}^1\text{H}$	21.6	-40.7	2.11	0.573	-3.8	2.80	0.931
3, ${}^4\text{He} + {}^3\text{He}$	23.4	-130.0	1.64	0.217	-1.8	2.12	0.700

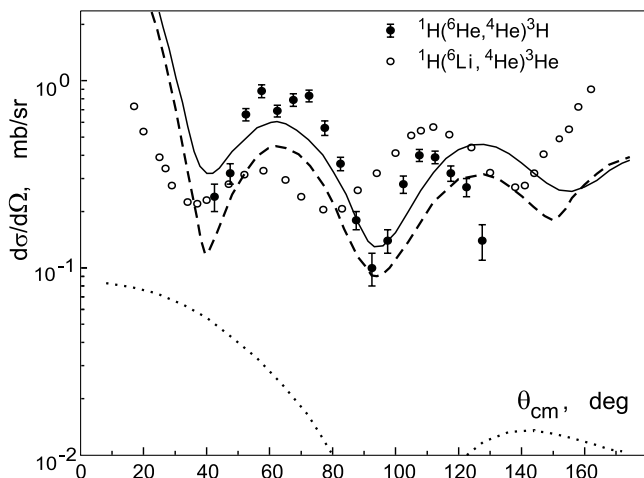


FIG. 4. Cross sections of the ${}^1\text{H}({}^6\text{He}, {}^4\text{He}){}^3\text{H}$ reaction at $E_{\text{c.m.}} = 21.6$ MeV (solid circles) and the ${}^6\text{Li}(p, {}^3\text{He}){}^4\text{He}$ reaction at $E_{\text{c.m.}} = 21.4$ MeV (open circles).

Three main differences between the two reactions can be seen. (i) The forward-backward angular asymmetry in the two reactions is opposite. Note that the dominant yield of ${}^3\text{He}$ at backward angles in the ${}^6\text{Li}(p, {}^3\text{He}){}^4\text{He}$ reaction is mainly due to transfer of ${}^3\text{H}$ from ${}^6\text{Li}$, whereas the deuteron transfer contributes mainly to the forward angle emission of ${}^3\text{He}$ in this reaction [9]. So, it seems (even without calculation) that ${}^3\text{H} + {}^3\text{H}$ clusterization of ${}^6\text{He}$ is less probable than the corresponding ${}^3\text{H} + {}^3\text{He}$ configuration in ${}^6\text{Li}$. (ii) The oscillations of the angular distribution in the ${}^1\text{H}({}^6\text{He}, {}^4\text{He}){}^3\text{H}$ reaction are much more pronounced than for the ${}^6\text{Li}(p, {}^3\text{He}){}^4\text{He}$ reaction. This may indicate a “purer” reaction mechanism and better l matching (zero angular momentum transfer) in the ${}^1\text{H}({}^6\text{He}, {}^4\text{He}){}^3\text{H}$ reaction, because a coherent sum of the contributions coming from different reaction mechanisms and sum over magnetic numbers of transferred angular momentum usually tend to smoothen an interference structure of the angular distributions in transfer reactions. (iii) The absolute value of the available $2n$ transfer cross section in the forward hemisphere in the ${}^1\text{H}({}^6\text{He}, {}^4\text{He}){}^3\text{H}$ reaction is slightly larger than the deuteron transfer cross section from the ${}^6\text{Li}$. This could be related to the more disperse $2n$ halo wave function in ${}^6\text{He}$ comparing with a more bound deuteron state in ${}^6\text{Li}$.

Data on elastic scattering of tritons from α particles at center-of-mass energies around 30 MeV do not seem to exist; hence we used available data on ${}^3\text{He} + {}^4\text{He}$ elastic scattering [10]. Fitting these data and data on ${}^6\text{He} + {}^1\text{H}$ elastic scattering [3] we found corresponding OM parameters (Table I), which were used in calculations of the $2n$ transfer reaction ${}^1\text{H}({}^6\text{He}, {}^4\text{He}){}^3\text{H}$ within our four-body approach. The ${}^3\text{H}$ bound state three-body wave function $\Psi_{3\text{H}}^{(134)}$ is not our main interest and was supposed to have a simple Jastrow form [11] with appropriate asymptotic behavior and a realistic value of the rms matter radius of ${}^3\text{H}$. Because of a short-range behavior the

function $\Psi_{3\text{H}}^{(134)}$ influences mainly an absolute value of the transfer cross section. The prior form of the transfer interaction ΔV was used with a proton- α interaction V_{12} taken from [12] and a p - n interaction of Gaussian shape with -45 MeV depth and 1.7 fm width. The calculated $2n$ transfer cross section is shown in Fig. 4 by the solid line, whereas the dashed and dotted lines show the contributions of the di-neutron and cigarlike configurations of ${}^6\text{He}$ to this process.

Comparison of calculated and experimental reaction cross sections and analysis of the $2n$ transfer reaction dynamics allow us to conclude that (i) the three-body n - n - α configuration of the ${}^6\text{He}$ nucleus has a weight close to unity; i.e., the spectroscopic factor $S_{(2n)\alpha}({}^6\text{He}) \approx 1$. (ii) The di-neutron component of this three-body configuration dominates in $2n$ transfer reactions induced by the Borromean nucleus ${}^6\text{He}$ at energies higher than 10 MeV/nucleon. This dominance is especially striking in the case of a hydrogen target. (iii) ${}^3\text{H} + {}^3\text{H}$ clusterization in ${}^6\text{He}$ seems to be much less probable compared with the ${}^3\text{H} + {}^3\text{He}$ configuration of ${}^6\text{Li}$.

Based on our encouraging findings we are presently pursuing studies of multinucleon transfer with a ${}^8\text{He}$ beam.

The authors acknowledge discussions with B. V. Danilin, S. N. Ershov, and M. V. Zhukov.

-
- [1] M. V. Zhukov, B. V. Danilin, D. V. Fedorov, J. M. Bang, I. J. Thompson, and J. S. Vaagen, *Phys. Rep.* **231**, 151 (1993).
 - [2] G. M. Ter-Akopian, A. M. Rodin, A. S. Fomichev, S. I. Sidorchuk, S. V. Stepanov, R. Wolski, M. L. Chelnokov, V. A. Gorshkov, A. Yu. Lavrentev, V. I. Zagrebaev, and Yu. Ts. Oganessian, *Phys. Lett. B* **426**, 251 (1998).
 - [3] R. Wolski, A. S. Fomichev, A. M. Rodin, S. I. Sidorchuk, S. V. Stepanov, G. M. Ter-Akopian, M. L. Chelnokov, V. A. Gorshkov, A. Yu. Lavrentev, V. I. Zagrebaev, and Yu. Ts. Oganessian, *JINR Report No. E15-98-284*, 1998.
 - [4] R. J. Ascutto and E. A. Seglie, in *Treatise on Heavy-Ion Science*, edited by D. A. Bromley (Plenum Press, New York, 1984), Vol. 1, p. 463.
 - [5] B. V. Danilin, M. V. Zhukov, A. A. Korshennikov, L. V. Chulkov, *Sov. J. Nucl. Phys.* **53**, 71 (1991).
 - [6] D. Bachelier, M. Bernas, J. L. Boyard, H. L. Harney, J. C. Jourdain, P. Radvanyi, M. Roy-Stephan, and R. Devries, *Nucl. Phys.* **A195**, 361 (1972).
 - [7] D. Baye, L. Desorgher, D. Guillaing, and D. Herschkowitz, *Phys. Rev. C* **54**, 2563 (1996).
 - [8] K. Schenk, M. Mörike, G. Staudt, P. Turek, and D. Clement, *Phys. Lett. B* **52**, 36 (1974).
 - [9] M. F. Werby, M. B. Greenfield, K. W. Kemper, D. L. McShan, and S. Edwards, *Phys. Rev. C* **8**, 106 (1973).
 - [10] R. Chiba, H. E. Conzett, H. Morinaga, N. Mutsuro, K. Shoda, and M. Kimura, *J. Phys. Soc. Jpn.* **16**, 1077 (1961).
 - [11] R. Jastrow, *Phys. Rev.* **98**, 1479 (1955).
 - [12] G. R. Satchler, L. W. Owe, A. J. Elwyn, G. L. Morgan, and R. L. Walter, *Nucl. Phys.* **A112**, 1 (1968).